PROCEEDINGS OF SCIENCE

Axion dark matter

Ilja Doršner[a,b,*]

[a] *University of Split, Faculty of Electrical Engineering, Mechanical Engineering and Naval Architecture, Ruđera Boškovića 32, 21000 Split, Croatia*

[b] *J. Stefan Institute, Jamova 39, P. O. Box 3000, 1001 Ljubljana, Slovenia*

E-mail: dorsner@fesb.hr

I present a minimal $SU(5)$ model with an additional $U(1)$ Peccei-Quinn symmetry that predicts the existence of an ultralight axion dark matter with a mass between 0.1 neV and 4.7 neV. I furthermore argue that the entire parameter space of the proposed model will be probed through a synergy between several low-energy experiments that look for proton decay (Hyper-Kamiokande), axion dark matter through axion-photon coupling (ABRACADABRA and DMRadio-GUT), and nucleon electric dipole moments (CASPEr Electric).

Proceedings of the Corfu Summer Institute 2024 "School and Workshops on Elementary Particle Physics and Gravity" (CORFU2024) 12 - 26 May, and 25 August - 27 September, 2024
Corfu, Greece

*Speaker

 ISSN 1824-8039 . Published by SISSA Medialab.

PoS(CORFU2024)222

1. Introduction

The simplest possible model of unification of the elementary particle interactions is the Georgi-Glashow model [1]. It embeds the entire Standard Model (SM) gauge group $SU(3)\times SU(2)\times U(1)$ within an $SU(5)$ framework. The Georgi-Glashow model, however, is not viable since (i) it fails to achieve gauge coupling unification, (ii) it predicts wrong mass relations between down-type quarks and charged leptons, and (iii) it yields massless neutrinos. Moreover, the Georgi-Glashow model does not address the strong CP problem, nor does it include a dark matter candidate.

The most compelling new physics resolution of the strong CP problem is given in terms of the Peccei-Quinn (PQ) symmetry [2, 3]. In the PQ framework, a global $U(1)_{\rm PQ}$ symmetry is spontaneously broken by a complex scalar leading to a nearly massless pseudoscalar particle [4–9], i.e., an "axion", which can serve as a cold dark matter candidate [10–12]. Since an axion can be embedded within the scalar representation that breaks the unification symmetry [13], I present a recent proposal [14] that combines the PQ symmetry with a simple, yet realistic, $SU(5)$ scenario [15, 16, 16] and showcase the main predictions of such a setup.

A detailed study [14] reveals that the proposed setup is highly predictive and that its entire parameter space will be fully tested through a combination of several experimental efforts. These comprise the proton decay experiment Hyper-Kamiokande as well as the axion dark matter experiments ABRACADABRA, DMRadio-GUT, and CASPEr Electric.

The manuscript is organized as follows. I introduce the particle content and symmetries of the model in Sec. 2. The details of the PQ symmetry implementation and the nature of the axion dark matter are discussed in detail in Sec. 3. A numerical study of the model is outlined in Sec. 4, where I also summarize the most relevant experimental predictions. I briefly conclude in Sec. 5.

2. The model

The model [14] comprises $\overline{5}_{F\,i}\equiv F_{\alpha\,i}$, $10_{F\,j}\equiv T_j^{\alpha\beta}=-T_j^{\beta\alpha}$, $\overline{15}_F\equiv\overline{\Sigma}_{\alpha\beta}=\overline{\Sigma}_{\beta\alpha}$, $15_F\equiv\Sigma^{\alpha\beta}$, $5_{H_a}\equiv\Lambda_a^\delta$ $(a=1,2)$, a complex $24_H\equiv\phi_\beta^\alpha$, $35_H\equiv\Phi_{\alpha\beta\gamma}$, and $24_V\equiv\Gamma_\beta^\alpha$, where Hs, Fs, and V denote whether a given irreducible representation, i.e., irrep, contains scalars, fermions, or gauge bosons, respectively, i,j $(=1,2,3)$ represent the generation indices, and $\alpha,\beta,\gamma,\delta$ $(=1,\ldots,5)$ are the $SU(5)$ indices. The decomposition of the $SU(5)$ scalar and fermion irreps under the SM gauge group $SU(3)\times SU(2)\times U(1)$ is presented in Table 1. I will refer to a given irrep/multiplet by using either its dimensionality with respect to the appropriate gauge group or the associated symbol. Beside the non-trivial assignment under the Lorentz symmetry, the aforementioned $SU(5)$ irreps carry the PQ $U(1)_{\rm PQ}$ charges that are presented in Table 2.

There are several parts of the scalar sector of the model that need to be discussed in detail. The $SU(5)\times U(1)_{\rm PQ}$ symmetry breaking is due to

$$\mathcal{L}\supset -\mu^2\phi_\alpha^{*\beta}\phi_\beta^\alpha+\xi_1(\phi_\alpha^{*\beta}\phi_\beta^\alpha)^2+\xi_2\phi_\alpha^{*\beta}\phi_\gamma^\alpha\phi_\delta^{*\gamma}\phi_\beta^\delta+\xi_3\phi_\alpha^{*\beta}\phi_\gamma^\delta\phi_\beta^{*\alpha}\phi_\delta^\gamma+\xi_4\phi_\alpha^{*\beta}\phi_\gamma^\delta\phi_\delta^{*\alpha}\phi_\beta^\gamma. \quad (1)$$

The VEV of ϕ_β^α that does the $SU(5)$ symmetry breaking reads

$$\langle\phi\rangle=\frac{v_\phi}{\sqrt{15}}{\rm diag}(-1,-1,-1,3/2,3/2), \quad (2)$$

$SU(5)$	$SU(3)\times SU(2)\times U(1)$	$SU(5)$	$SU(3)\times SU(2)\times U(1)$
$5_{H_a}\equiv\Lambda_a^\alpha$	$\Xi_a\left(1,2,+\frac{1}{2}\right)$ $\omega_a\left(3,1,-\frac{1}{3}\right)$	$\overline{5}_{Fi}\equiv F_{\alpha i}$	$L_i\left(1,2,-\frac{1}{2}\right)$ $d_i^c\left(\overline{3},1,+\frac{1}{3}\right)$
$24_H\equiv\phi_\beta^\alpha$	$\phi_0\,(1,1,0)$ $\phi_1\,(1,3,0)$ $\phi_3\left(3,2,-\frac{5}{6}\right)$ $\phi_{\overline{3}}\left(\overline{3},2,+\frac{5}{6}\right)$ $\phi_8\,(8,1,0)$	$10_{Fi}\equiv T_i^{\alpha\beta}$	$Q_i\left(3,2,+\frac{1}{6}\right)$ $u_i^c\left(\overline{3},1,-\frac{2}{3}\right)$ $e_i^c\,(1,1,+1)$
		$\overline{15}_F\equiv\overline{\Sigma}_{\alpha\beta}$	$\overline{\Sigma}_1(1,3,-1)$ $\overline{\Sigma}_3\left(\overline{3},2,-\frac{1}{6}\right)$ $\overline{\Sigma}_6\left(\overline{6},1,+\frac{2}{3}\right)$
$35_H\equiv\Phi_{\alpha\beta\gamma}$	$\Phi_1\left(1,4,-\frac{3}{2}\right)$ $\Phi_3\left(\overline{3},3,-\frac{2}{3}\right)$ $\Phi_6\left(\overline{6},2,+\frac{1}{6}\right)$ $\Phi_{10}\left(\overline{10},1,+1\right)$	$15_F\equiv\Sigma^{\alpha\beta}$	$\Sigma_1\,(1,3,+1)$ $\Sigma_3\left(3,2,+\frac{1}{6}\right)$ $\Sigma_6\left(6,1,-\frac{2}{3}\right)$

Table 1: Content and nomenclature of the scalar and fermion irreps of the proposal at both the $SU(5)$ and SM levels. $\alpha,\beta,\gamma\,(=1,\ldots,5)$ are the $SU(5)$ indices, $i(=1,2,3)$ is a generation index, and $a(=1,2)$ refers to two copies of scalars in the fundamental representation.

$SU(5)$ irrep	$\overline{5}_{Fi}$	10_{Fi}	$\overline{15}_F$	15_F	5_{H_1}	5_{H_2}	24_H	35_H	24_V
$U(1)_{\rm PQ}$ charge	$-\frac{1}{2}$	$-\frac{1}{2}$	$-\frac{1}{2}$	$-\frac{1}{2}$	-1	$+1$	$+1$	-1	0

Table 2: $U(1)_{\rm PQ}$ charge assignment of the model. H, F, and V subscripts denote scalar, fermion, or gauge boson $SU(5)$ irreps, respectively, while $i=1,2,3$.

multiplet	real part mass-squared	imaginary part mass-squared
$\phi_0\,(1,1,0)$	m_1^2	0
$\phi_1\,(1,3,0)$	m_3^2	$\frac{1}{4}m_3^2+m_8^2$
$\phi_8\,(8,1,0)$	$\frac{1}{4}m_3^2$	m_8^2
$\phi_3\left(3,2,-\frac{5}{6}\right)$	0	$m_{5/6}^2$
$\phi_{\overline{3}}\left(\overline{3},2,+\frac{5}{6}\right)$	0	$m_{5/6}^2$

Table 3: Mass-squared spectrum of a complex irrep $24_H\equiv\phi$.

where I assume that the VEV of the electrically neutral component of the $SU(2)$ triplet $\phi_1(\in 24_H)$ is negligible. The squares of masses of multiplets in 24_H, as generated via Eqs. (1) and (2), are summarized in Table 3 for convenience.

The potential given by Eq. (1) dictates that the imaginary part of $\phi_0(\in 24_H)$ is massless. In fact, the axion is mostly composed of that particular state, as I discuss later on. The real components of $\phi_3(\in 24_H)$ and $\phi_{\overline{3}}(\in 24_H)$, on the other hand, provide the necessary degrees of freedom for the

proton decay mediating gauge bosons in 24_V to obtain a mass $M_{\rm GUT}$, where

$$M^2_{\rm GUT} = \frac{5\pi}{6}\alpha_{\rm GUT} v^2_\phi . \tag{3}$$

Here, $M_{\rm GUT}$ is also the scale of gauge coupling unification, and $\alpha_{\rm GUT}$ is the corresponding $SU(5)$ gauge coupling constant.

The scalar fields in the fundamental irreps of $SU(5)$ couple via

$$\mathcal{L} \supset \sum_{a=1}^{2} \left\{ -\frac{1}{2}\mu^2_{\Lambda_a}\Lambda^\dagger_a\Lambda_a + \gamma_{\Lambda_a}\left(\Lambda^\dagger_a\Lambda_a\right)^2 \right\} + \zeta_1\left(\Lambda^\dagger_1\Lambda_1\right)\left(\Lambda^\dagger_2\Lambda_2\right) + \zeta_2\left(\Lambda^\dagger_1\Lambda_2\right)\left(\Lambda^\dagger_2\Lambda_1\right) , \tag{4}$$

where I suppress $SU(5)$ indices. The doublet-triplet spitting, i.e., breaking of the mass degeneracy between Ξ_a and ω_a, is accomplished via the following additional terms in the scalar potential

$$\mathcal{L} \supset \sum_{a=1}^{2} \left\{ \lambda_{\Lambda_a}\Lambda^\dagger_a\Lambda_a\phi^\dagger\phi + \Lambda^\dagger_a\left(\alpha_{\Lambda_a}\phi^\dagger\phi + \beta_{\Lambda_a}\phi\phi^\dagger\right)\Lambda_a \right\} + \left\{ \kappa_1\Lambda^\dagger_2\phi^2\Lambda_1 + \kappa_2\left(\Lambda^\dagger_2\Lambda_1\right)\phi^2 + \text{h.c.} \right\}.$$

The mass-squared matrices of ω_a and Ξ_a multiplets, in the Λ_1-Λ_2 basis, are

$$M^2_\omega = \begin{pmatrix} -\mu^2_{\Lambda_1} + \frac{v^2_\phi}{15}\left(2\alpha_{\Lambda_1} + 2\beta_{\Lambda_1} + 15\lambda_{\Lambda_1}\right) & v^2_\phi\left(\frac{2}{15}\kappa_1 + \kappa_2\right) \\ v^2_\phi\left(\frac{2}{15}\kappa_1 + \kappa_2\right) & -\mu^2_{\Lambda_2} + \frac{v^2_\phi}{15}\left(2\alpha_{\Lambda_2} + 2\beta_{\Lambda_2} + 15\lambda_{\Lambda_2}\right) \end{pmatrix}, \tag{5}$$

$$M^2_\Xi = \begin{pmatrix} -\mu^2_{\Lambda_1} + \frac{v^2_\phi}{10}\left(3\alpha_{\Lambda_1} + 3\beta_{\Lambda_1} + 10\lambda_{\Lambda_1}\right) & v^2_\phi\left(\frac{3}{10}\kappa_1 + \kappa_2\right) \\ v^2_\phi\left(\frac{3}{10}\kappa_1 + \kappa_2\right) & -\mu^2_{\Lambda_2} + \frac{v^2_\phi}{10}\left(3\alpha_{\Lambda_2} + 3\beta_{\Lambda_2} + 10\lambda_{\Lambda_2}\right) \end{pmatrix}. \tag{6}$$

Clearly, the required doublet-triplet splitting can be obtained by an appropriate choice of the model parameters. The linear combinations of ω_1 and ω_2 will consequently yield mass eigenstates I denote T_1 and T_2 in the rest of the manuscript. Also, Ξ_1 and Ξ_2 will produce mass eigenstates H_1 and H_2, where H_1 is identified with the SM Higgs with 125 GeV mass.

Finally, the VEVs of 5_{H_a} that break $SU(3)\times SU(2)\times U(1)$ down to $SU(3)\times U(1)_{\rm em}$ are $\langle\Lambda_a\rangle = (0 \quad 0 \quad 0 \quad 0 \quad v_{\Lambda_a})^T$.

The lepton number conservation is violated via a single term in the Lagrangian that reads

$$\mathcal{L} \supset \lambda\Lambda^\alpha_1\Lambda^\beta_2\Lambda^\gamma_2\Phi_{\alpha\beta\gamma} + \text{h.c.}. \tag{7}$$

The neutrino masses will thus be directly proportional to the dimensionless parameter λ of Eq. (7).

The masses of the SM multiplets in 35_H are determined by the following $SU(5)$ contractions

$$\mathcal{L} \supset \mu^2_{35}\Phi\Phi^* + \lambda_0\left(\Phi\Phi^*\right)\phi^*\phi + \lambda_1\Phi_{\alpha\beta\gamma}(\Phi^*)^{\alpha\delta\epsilon}(\phi^*)^\beta_\delta\phi^\gamma_\epsilon + \lambda_2\Phi_{\alpha\beta\epsilon}(\Phi^*)^{\alpha\beta\delta}(\phi^*)^\epsilon_\gamma\phi^\gamma_\delta . \tag{8}$$

These contractions yield

$$M^2_{\Phi_1} = \mu^2_{35} + v^2_\phi\left(\frac{\lambda_0}{2} + \frac{3\lambda_1}{20} + \frac{3\lambda_2}{20}\right), \tag{9}$$

$$M^2_{\Phi_3} = \mu^2_{35} + v^2_\phi\left(\frac{\lambda_0}{2} - \frac{\lambda_1}{60} + \frac{11\lambda_2}{90}\right), \tag{10}$$

$$M^2_{\Phi_6} = \mu^2_{35} + v^2_\phi\left(\frac{\lambda_0}{2} - \frac{2\lambda_1}{45} + \frac{17\lambda_2}{180}\right), \tag{11}$$

$$M^2_{\Phi_{10}} = \mu^2_{35} + v^2_\phi\left(\frac{\lambda_0}{2} + \frac{\lambda_1}{15} + \frac{1\lambda_2}{15}\right). \tag{12}$$

These, in turn, produce a single mass-squared relation that reads

$$M^2_{\Phi_{10}} = M^2_{\Phi_1} - 3M^2_{\Phi_3} + 3M^2_{\Phi_6}. \tag{13}$$

The mass spectrum given in Table 3 and the mass relation presented in Eq. (13) are necessary input for the gauge coupling unification analysis.

The Yukawa sector of the model is

$$\begin{aligned}\mathcal{L} \supset\ & Y^u_{ij}\ 10_{F\,i}10_{F\,j}5_{H_2} + Y^d_{ij}\ 10_{F\,i}\overline{5}_{F\,j}5^*_{H_1} + Y^a_i\ 15_F\overline{5}_{F\,i}5^*_{H_1} \\ & + Y^b_i\ \overline{15}_F\overline{5}_{F\,i}35^*_H + Y^c_i\ 10_{F\,i}\overline{15}_F24_H + y\ \overline{15}_F15_F24_H + \text{h.c.},\end{aligned} \tag{14}$$

where the PQ charge assignment of Table 2 and the $SU(5)$ indices are all implicitly understood. The Yukawa matrix elements of the model are $Y^u_{ij} \equiv Y^u_{ji}$, $Y^d_{ij} = Y^{d*}_{ij} \equiv \delta_{ij}Y^d_i$, Y^a_i, Y^b_i, Y^c_i, and y, where I have used the freedom to rotate irreps in the $SU(5)$ group space to reach this particular Yukawa coupling basis.

The PQ charge assignment forbids a bare-mass term for the $\overline{15}_F$-15_F pair. The masses of the associated SM multiplets are thus generated solely through the last term of Eq. (14), which reads

$$\mathcal{L} \supset \frac{yv_\phi}{\sqrt{15}}\left(\frac{3}{2}\overline{\Sigma}_1\Sigma_1 + \frac{1}{4}\overline{\Sigma}_3\Sigma_3 - \overline{\Sigma}_6\Sigma_6\right) + \text{h.c.}, \tag{15}$$

where the overall phase of 24_H is not shown for simplicity. I subsequently define

$$M_{\Sigma_1} = \frac{y}{2}\sqrt{\frac{3}{5}}v_\phi\,, \tag{16}$$

$$M_{\Sigma_3} = \frac{y}{4\sqrt{15}}v_\phi\,, \tag{17}$$

$$M_{\Sigma_6} = -\frac{y}{\sqrt{15}}v_\phi. \tag{18}$$

The masses of the SM fermions are obtained after the breaking of the SM gauge group down to $SU(3)\times U(1)_{\rm em}$ as follows. The down-type quark sector 4×4 mass matrix can be written as

$$M_D = \begin{pmatrix} v_{\Lambda_1}Y^d & v'_\phi Y^c \\ v_{\Lambda_1}Y^a & M_{\Sigma_3}\end{pmatrix}, \tag{19}$$

where I introduce $v'_\phi = -\frac{1}{4}\sqrt{\frac{5}{3}}v_\phi$. This matrix can be transformed into a block-diagonal form comprising a 3×3 part denoted M_d and a mass parameter M_H as follows

$$XM_DY^\dagger = \begin{pmatrix} M_d & 0 \\ 0 & M_H\end{pmatrix}, \tag{20}$$

where unitary matrices X and Y take the form

$$X \sim \begin{pmatrix} \left(1 + \frac{v'^2_\phi}{M^2_{\Sigma_3}}Y^cY^{c\dagger}\right)^{-1/2} & -\left(1 + \frac{v'^2_\phi}{M^2_{\Sigma_3}}Y^cY^{c\dagger}\right)^{-1/2}\frac{v'_\phi}{M_{\Sigma_3}}Y^c \\ \frac{v'_\phi Y^{c\dagger}}{M_H} & \frac{M_{\Sigma_3}}{M_H}\end{pmatrix}, \tag{21}$$

$$Y \sim \begin{pmatrix} 1 & -\frac{v_{\Lambda_1}v'_\phi}{M^2_H}(Y^{d\dagger}Y^c + \frac{M_{\Sigma_3}}{v'_\phi}Y^{a\dagger}) \\ \frac{v_{\Lambda_1}v'_\phi}{M^2_H}(Y^{c\dagger}Y^d + \frac{M_{\Sigma_3}}{v'_\phi}Y^a) & 1\end{pmatrix}, \tag{22}$$

with

$$M_d \sim \left(1 + \frac{v'^2_\phi}{M^2_{\Sigma_3}} Y^c Y^{c\,\dagger}\right)^{-1/2} \left(v_{\Lambda_1} Y^d - \frac{v_{\Lambda_1} v'_\phi}{M_{\Sigma_3}} Y^c Y^a\right), \tag{23}$$

$$M_H = \sqrt{M^2_{\Sigma_3} + v'^2_\phi Y^{c\,\dagger} Y^c} \approx M_{\Sigma_3}. \tag{24}$$

Here, $1 = \text{diag}(1,1,1)$ while Y^c, Y^a, and Y^d are Yukawa matrices that are featured in Eq. (14). It is clear from Eq. (23) that the down-type quark mass matrix M_d is generated through the VEV of 5_{H_1} and the mixing between fields in $\overline{5}_{F\,i}$, $10_{F\,i}$, $\overline{15}_F$, and 15_F.

The charged fermion mass matrices of the model can be succinctly written as

$$M_u = \left(1 + \delta^2\, Y^c Y^{c\,\dagger}\right)^{-\frac{1}{2}} 8 v_{\Lambda_2} Y^u, \tag{25}$$

$$M_d = \left(1 + \delta^2\, Y^c Y^{c\,\dagger}\right)^{-\frac{1}{2}} v_{\Lambda_1} \left(Y^d + \delta\, Y^c Y^a\right), \tag{26}$$

$$M_e = v_{\Lambda_1} Y^d, \tag{27}$$

where $\delta = -v'_\phi / M_{\Sigma_3}$ and $v^2_{\Lambda_1} + v^2_{\Lambda_2} = v^2$ with $v = 174\,\text{GeV}$. I note the two most prominent features of the charged fermion sector. First, M_u can be treated as a symmetric matrix in the flavor space. Second, a mismatch between the charged lepton and down-type quark mass matrices is proportional to a rank-one matrix $Y^c Y^a$. Again, I work in the basis where $Y^u_{ij} \equiv Y^u_{ji}$ and $Y^d_{ij} = Y^{d*}_{ij} \equiv \delta_{ij} Y^d_i$. This simply means that $v_{\Lambda_1} Y^d{}_i$, where $i = 1,2,3$, are the masses of the SM charged leptons.

The neutrino mass in this model is generated by utilizing the Yukawa couplings Y^a and Y^b that appear in Eq. (14) and the lepton number violating term of Eq. (7). Completion of the neutrino mass loop requires, in addition to the SM fields, the presence of $(1,3,1) + (1,3,-1) (\subset 15_F + \overline{15}_F)$ vectorlike fermions and the scalar quadruplet $(1,4,-3/2) (\subset 35_H)$. The corresponding Feynman diagram illustrating the neutrino mass generation mechanism [17, 18] is shown in Fig. 1.

The neutrino mass matrix elements $(M_\nu)_{ij}$, at the leading order, read

$$\begin{aligned}(M_\nu)_{ij} &\approx \frac{\lambda v^2_{\Lambda_2}}{8\pi^2} (Y^a_i Y^b_j + Y^b_i Y^a_j) \frac{M_{\Sigma_1}}{M^2_{\Sigma_1} - M^2_{\Phi_1}} \ln\left(\frac{M^2_{\Sigma_1}}{M^2_{\Phi_1}}\right) \\ &\equiv m_0 (Y^a_i Y^b_j + Y^b_i Y^a_j) = (N\, \text{diag}(0, m_2, m_3)\, N^T)_{ij}\,,\end{aligned} \tag{28}$$

where m_2 and m_3 are neutrino mass eigenstates and N is a unitary matrix. One of the neutrinos is a strictly massless particle due to the fact that M_ν is constructed out of two rank-one matrices with elements $Y^a_i Y^b_j$ and $Y^b_i Y^a_j$.

Since the charged lepton mass matrix in Eq. (27) is already in a diagonal form, N reads

$$N = \text{diag}(e^{i\eta^\nu_1}, e^{i\eta^\nu_2}, e^{i\eta^\nu_3}) V^*_{\text{PMNS}}, \tag{29}$$

where V_{PMNS} is the Pontecorvo-Maki-Nakagawa-Sakata (PMNS) unitary mixing matrix, that is defined as $V_{\text{PMNS}} = R_{23} U_{13} R_{12} Q$, with $Q = \text{diag}(1, e^{i\beta^\nu}, 1)$. Here, I use the PDG parametrization [19] for the R_{23}, U_{13}, and R_{12} matrices. Note that there is only one Majorana phase β^ν in Q due to the fact that one of the neutrinos is massless.

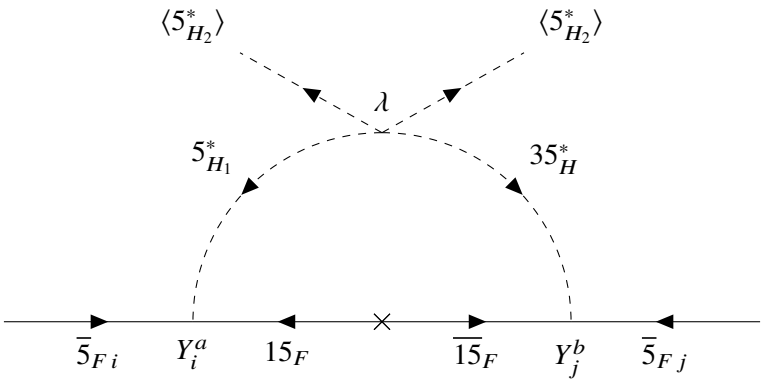

Figure 1: The one-loop Feynman diagram which is responsible for neutrino mass generation.

Matrices Y^a and Y^b can be expressed in terms of the PMNS matrix parameters and phases η^ν_i, $i = 1, 2, 3$, in the following form [20, 21]

$$Y^{a\,T} = \frac{\xi}{\sqrt{2}}\begin{pmatrix} i\, r_2\, N_{12} + r_3\, N_{13} \\ i\, r_2\, N_{22} + r_3\, N_{23} \\ i\, r_2\, N_{32} + r_3\, N_{33} \end{pmatrix}, \quad Y^{b\,T} = \frac{1}{\sqrt{2}\xi}\begin{pmatrix} -i\, r_2\, N_{12} + r_3\, N_{13} \\ -i\, r_2\, N_{22} + r_3\, N_{23} \\ -i\, r_2\, N_{32} + r_3\, N_{33} \end{pmatrix}, \tag{30}$$

where N_{ij} denotes the ij-th element of the unitary matrix N, $r_2 = \sqrt{m_2/m_0}$, and $r_3 = \sqrt{m_3/m_0}$. Moreover, ξ is a dimensionless scaling parameter that allows one to accurately scan over all possible viable entries in Y^a and Y^b that accommodate experimental observables in the neutrino sector.

3. Peccei-Quinn symmetry and axion dark matter

The VEV of $24_H \equiv \phi^\alpha_\beta$ can be written as [13]

$$\langle\phi\rangle = \frac{\hat{v}_\phi}{\sqrt{2}}\text{diag}\left(\frac{-1}{\sqrt{15}}, \frac{-1}{\sqrt{15}}, \frac{-1}{\sqrt{15}}, \frac{3}{2\sqrt{15}}, \frac{3}{2\sqrt{15}}\right) e^{i a_\phi(x)/\hat{v}_\phi}, \quad \hat{v}_\phi \equiv \sqrt{2} v_\phi, \tag{31}$$

where the pseudoscalar part, i.e., field $a_\phi(x)$, essentially remains massless, whereas the radial mode acquires a mass of the order of the unification scale while the global $U(1)_{\rm PQ}$ symmetry is spontaneously broken with order parameter v_ϕ. To correctly identify the massless axion, one also needs to include all other Higgses that carry PQ charges and participate in symmetry breaking.

The VEVs of neutral components of the $SU(2)$ doublets can be re-written as

$$\langle\Lambda_2\rangle = \frac{\hat{v}_{\Lambda_2}}{\sqrt{2}} e^{i\frac{a_{\Lambda_2}}{\hat{v}_{\Lambda_2}}}, \quad \langle\Lambda_1^*\rangle = \frac{\hat{v}_{\Lambda_1}}{\sqrt{2}} e^{i\frac{a_{\Lambda_1}}{\hat{v}_{\Lambda_1}}}, \quad \hat{v}_{\Lambda_a} \equiv \sqrt{2} v_{\Lambda_a}, \tag{32}$$

where I take all VEVs to be real. With these assumptions, the axion field is identified as [22],

$$a = \frac{x_{\Lambda_2}\hat{v}_{\Lambda_2} a_{\Lambda_2} + x^*_{\Lambda_1}\hat{v}_{\Lambda_1} a_{\Lambda_1} + x_\phi \hat{v}_\phi a_\phi}{v_a}, \quad v_a^2 = x^2_{\Lambda_2}\hat{v}^2_{\Lambda_2} + x^2_{\Lambda_1}\hat{v}^2_{\Lambda_1} + x^2_\phi \hat{v}^2_\phi, \tag{33}$$

where x_i denotes the PQ charge of the corresponding i-th scalar (and $x^*_i = -x_i$). Since $v_\phi \sim 10^{16}$ GeV and $v_{\Lambda_a} \sim 10^2$ GeV, the axion mostly resides in 24_H with $a \approx a_\phi$.

The axion field must also be orthogonal to the Goldstone field eaten up by the Z-boson. This translates into the following condition

$$\tan^2\beta = v_{\Lambda_2}^2/v_{\Lambda_1}^2 = x_{\Lambda_1}^*/x_{\Lambda_2}, \tag{34}$$

which yields $\tan\beta = 1$.

Now, performing a field-dependent axial transformation that is anomalous under QCD, the axion can be disentangled from the Yukawa interactions. This transformation generates the effective anomalous interactions of the following types:

$$\delta\mathcal{L}_{\rm eff} = \frac{\alpha_s}{8\pi}\frac{a}{f_a}G\widetilde{G} + \left(\frac{\alpha_{\rm em}}{2\pi f_a}\frac{\mathcal{E}}{\mathcal{N}}\right)\frac{a}{4}F\widetilde{F}\ . \tag{35}$$

Here, G (F) is the gluon (photon) field strength tensor, $\widetilde{G}$ ($\widetilde{F}$) is its dual, and f_a is the axion decay constant. The effective operator of the form $aG\widetilde{G}$ is the key to the PQ solution to the strong CP problem. Since these sub-multiplets carry color and electromagnetic charges, the PQ current has both QCD and electromagnetic anomalies, with the corresponding anomaly coefficients [23],

$$\mathcal{N} = \sum_\psi N_\psi, \quad \mathcal{E} = \sum_\psi E_\psi\ , \tag{36}$$

where sums run over all fermions generically denoted by ψ. Using well-known formulas,

$$N_\psi = x_\psi d(I_\psi)T(C_\psi), \tag{37}$$

$$E_\psi = x_\psi d(C_\psi)d(I_\psi)\left(\frac{1}{12}(d(I_\psi)^2-1)+Y_\psi^2\right), \tag{38}$$

I obtain $|\mathcal{N}| \equiv \hat{\mathcal{N}} = 13/2$ and $|\mathcal{E}| \equiv \hat{\mathcal{E}} = 52/3$ while the domain-wall number, which is relevant for cosmology, is $N_{\rm DW} = 2\hat{\mathcal{N}} = 13$. Subsequently, the axion decay constant is found to be

$$f_a = \frac{v_a}{2\hat{\mathcal{N}}} \approx \frac{\hat{v}_\phi}{2\hat{\mathcal{N}}} = \sqrt{\frac{3}{10\pi\alpha_{\rm GUT}}}\frac{M_{\rm GUT}}{\hat{\mathcal{N}}}. \tag{39}$$

Once strong interactions confine, non-perturbative QCD effects generate a potential that gives rise to a tiny axion mass [24, 25]

$$m_a = 5.7\,{\rm neV}\left(\frac{10^{15}\,{\rm GeV}}{f_a}\right) = 5.7\,{\rm neV}\left(\frac{10^{15}\,{\rm GeV}}{M_{\rm GUT}}\right)\hat{\mathcal{N}}\sqrt{\frac{10\pi\alpha_{\rm GUT}}{3}}\ . \tag{40}$$

This shows that the axion mass is predicted if the grand unification scale $M_{\rm GUT}$ is known.

Since the non-observation of proton decay requires $M_{\rm GUT}$ to be large, the axion mass is expected to be around the neV scale within this setup. Remarkably, an axion with neV mass can serve as an excellent dark matter candidate and can be searched for efficiently in direct detection experiments [29] hunting for ultra-light axions.

Next, I consider the most relevant axion couplings for experimental sensitivity. In the low-energy effective Lagrangian for the axion, it is sometimes convenient to eliminate the axion coupling

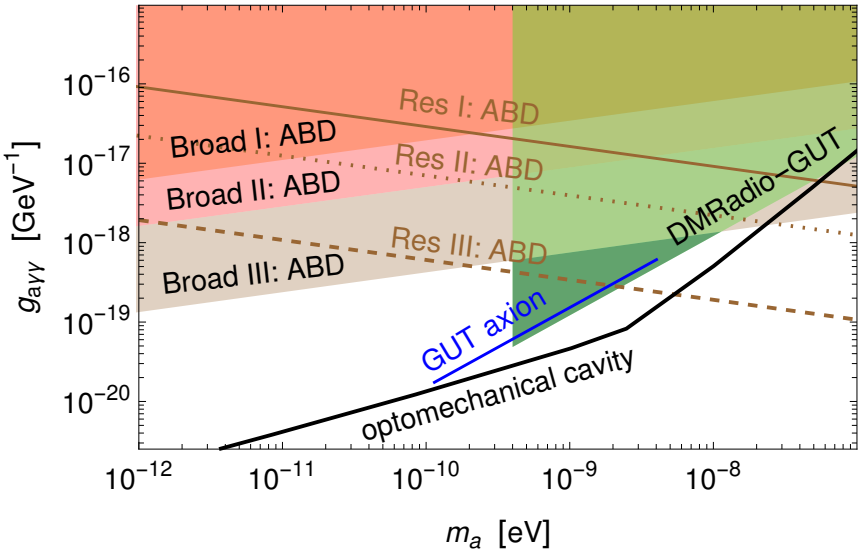

Figure 2: Expected reach in the m_a vs. $g_{a\gamma\gamma}$ plane for the broadband (Broad) and resonant (Res) strategies of the ABRACADABRA (ABD) experiment [26]. The blue line corresponds to the prediction of the model. The projected $3\,\sigma$ sensitivity of DMRadio-GUT [27] is also presented in the green shaded region. Furthermore, the expected theoretical reach using the optomechanical cavity method [28] is shown with solid black lines.

to the gluons via a field-dependent axial transformation of the SM quarks. After making such a rotation, the axion coupling to the photons is given by [25],

$$\mathcal{L} \supset \underbrace{\frac{\alpha_{\rm em}}{2\pi f_a}\left(\frac{\hat{\mathcal{E}}}{\hat{\mathcal{N}}} - 1.92\right)}_{\equiv g_{a\gamma\gamma}} \frac{a}{4} F\widetilde{F}, \tag{41}$$

where the model-dependent quantity, apart from f_a (see Eq. (39)) is given by $\hat{\mathcal{E}}/\hat{\mathcal{N}} = 8/3$. In fact, the dark matter experiment ABRACADABRA [26] has a great potential to look for an axion dark matter in the mass range of interest. As shown in Fig. 2, a major part of the parameter space will be probed by this dark matter direct detection experiment. Fig. 2 is obtained by varying the model parameters while imposing all relevant constraints.

Another axion dark matter experiment, the DMRadio-GUT [27], will also be sensitive in detecting axions with GUT scale decay constant $f_a (\sim 10^{16}\,\text{GeV})$. DMRadio-GUT will be far more sensitive compared to its previous two phases, i.e., DMRadio-50L and DMRadio-m^3, since it will have a factor of three enhancement in the field and a factor of ten enhancement in volume relative to DMRadio-m^3. The projected $3\,\sigma$ sensitivity of DMRadio-GUT is also presented in Fig. 2 by a green shaded region, which will probe a significant portion of the parameter space. Yet another proposal utilizing an optomechanical cavity [28] filled with superfluid helium is shown to be highly promising in detecting ultra-light axion dark matter. In Fig. 2, the corresponding theoretical reach is shown with solid black lines. The ABRACADABRA experiment will be sensitive to axion masses as low as $m_a \sim 2\,\text{neV}$, whereas the sensitivity of DMRadio-GUT and optomechanical cavity is about $m_a \sim 0.4\,\text{neV}$ and $m_a \sim 0.1\,\text{neV}$, respectively. A combination of all these axion dark matter experiments will eventually probe the entire parameter space of the proposed model.

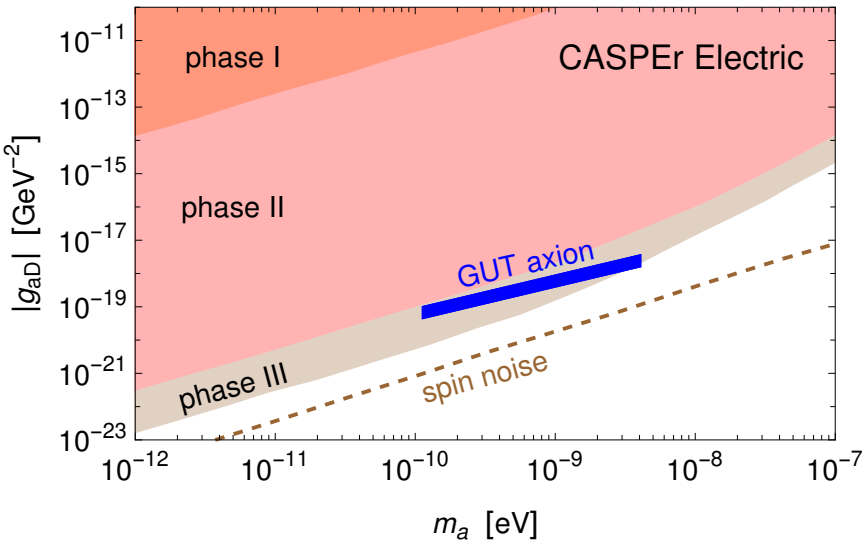

Figure 3: Axion coupling to the nucleon EDM operator as a function of the axion mass. The blue band corresponds to the prediction of the model. The shaded regions show the sensitivity projections of CASPEr Electric [30, 31] in its various phases. The ultimate sensitivity limit is given by the nuclear spin noise.

Intriguingly, ultra-light axion dark matter can also be efficiently searched for via oscillating nucleon electric dipole moments (EDM). As already stated, the QCD axion solves the strong CP problem by promoting the θ parameter into the dynamical axion field. Consequently, the effective θ angle gives rise to an EDM for nucleons sourced by the axion. Owing to the dynamical nature of the axion, this EDM will change in time, giving rise to unique signals. In the effective Lagrangian, the coupling of the axion to nucleon n takes the following form,

$$\mathcal{L} \supset -\frac{i}{2} g_{aD}\, a\, \overline{\psi}_n \sigma_{\mu\nu}\gamma_5 \psi_n F^{\mu\nu} \,. \tag{42}$$

The nucleon electric dipole moment generated through the above operator is given by $d_n = g_{aD} a$. The classical field that describes the axion field can be written as $a = a_0 \cos(m_a t)$. The amplitude, a_0, is determined from the local dark matter density, namely, $\rho_{\rm DM} = \frac{1}{2} m_a^2 a_0^2$, which assumes the axion comprises 100% of dark matter within this setup. The nucleon electric dipole moment is then determined by the dark matter energy density, $d_n = \sqrt{2} g_{aD} \sqrt{\rho_{\rm DM}} \cos(m_a t)/m_a$. Moreover, the nucleon electric dipole moment can also be expressed in terms of the axion decay constant. In terms of the model parameters, it can be re-written in the following form [32]:

$$d_n \approx a \underbrace{\frac{2.4 \times 10^{-16}}{f_a}}_{g_{aD}} e \cdot \text{cm}, \tag{43}$$

with roughly a 40% uncertainty [33], where the decay constant is given in Eq. (39). The corresponding coupling as a function of the axion mass is shown in Fig. 3. As can be seen from this figure, excitingly, the CASPEr Electric [30, 31] experiment alone will probe almost the entire parameter space of the model. Fig. 3 is also obtained by varying model parameters after one imposes all the relevant constraints. The exact details will be discussed later in the text.

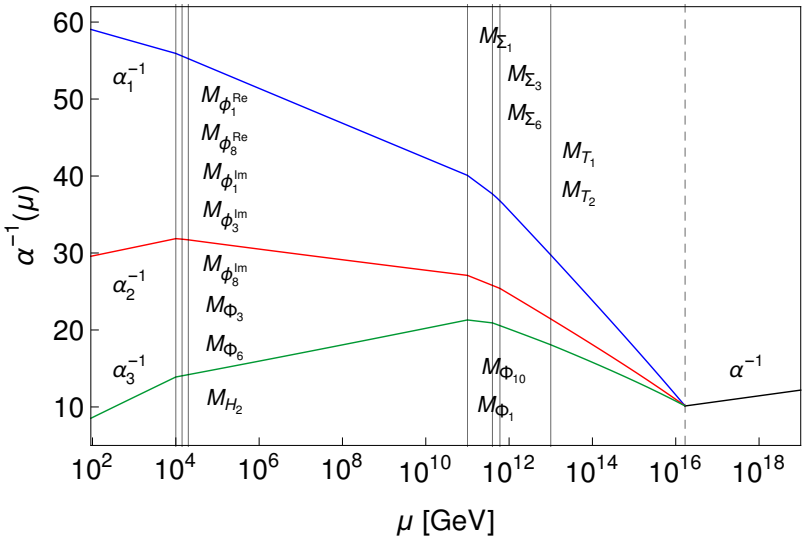

Figure 4: Example for the choice of the intermediate-scale particle masses giving gauge coupling unification.

Since the axion is ultra-light in this setup, it can constitute the entirety of the dark matter. I assume that the $U(1)_{\rm PQ}$ remains broken during inflation and is never restored afterwards. In such a scenario, the relic abundance of the axion dark matter is given by [34]

$$\Omega h^2 \sim 0.12 \left(\frac{5\,\text{neV}}{m_a}\right)^{1.17} \left(\frac{\theta_i}{1.53\times 10^{-2}}\right)^2 , \tag{44}$$

which shows that the initial value of $\theta_i = a_i/f_a$, where a_i is the value of the axion field, needs to be somewhat smaller than unity to be consistent with the observed dark matter relic abundance $\Omega h^2 \sim 0.12 \pm 0.001$ [35]. Thus, for $\theta_i \sim 10^{-2}$, the axion is composed of all the dark matter.

4. Unification, axion mass and proton decay

In this model [14], the axion decay width f_a is connected to the unification scale $M_{\rm GUT}$ due to the fact that 24_H simultaneously breaks the $SU(5)$ and $U(1)_{\rm PQ}$ symmetries. This, in particular, directly relates the axion mass m_a to the GUT scale $M_{\rm GUT}$ via Eq. (40). Moreover, since the partial proton lifetimes are proportional to the fourth power of $M_{\rm GUT}$, the model can be simultaneously probed with axion dark matter and proton decay experiments.

In order to investigate the viable part of the parameter space giving gauge coupling unification, the masses of the fields $\phi_1^{\rm Re}$, $\phi_1^{\rm Im}$, $\phi_3^{\rm Im}$, $\phi_8^{\rm Re}$, $\phi_8^{\rm Im}$, Σ_1, Σ_3, Σ_6, Φ_1, Φ_3, Φ_6, Φ_{10}, and H_2 are freely varied between the TeV and the GUT scale, while taking into account the mass spectrum constraints presented in Sec. 2. To ensure that the scalar leptoquark mediated proton decay is sufficiently suppressed, the masses of T_1 and T_2 are varied between 3×10^{11} GeV and the GUT scale. The low-scale values used as an input are $g_1 = 0.461425^{+0.000044}_{-0.000043}$, $g_2 = 0.65184^{+0.00018}_{-0.00017}$, and $g_3 = 1.2143^{+0.0035}_{-0.0036}$ [36], where $g_i = \sqrt{4\pi\alpha_i}$. To demonstrate how the gauge coupling unification works, I show in Fig. 4 one possible mass spectrum giving gauge coupling unification that agrees with the proton decay constraints and that yields correct neutrino mass scale via Eq. (28).

decay channel	current bound τ_p [yrs]	future sensitivity τ_p [yrs]
$p \to \pi^0 e^+$	$2.4 \cdot 10^{34}$ [37]	$7.8 \cdot 10^{34}$ [38]
$p \to \pi^0 \mu^+$	$1.6 \cdot 10^{34}$ [37]	$7.7 \cdot 10^{34}$ [38]
$p \to \eta^0 e^+$	$1.0 \cdot 10^{34}$ [39]	$4.3 \cdot 10^{34}$ [38]
$p \to \eta^0 \mu^+$	$4.7 \cdot 10^{33}$ [39]	$4.9 \cdot 10^{34}$ [38]
$p \to K^0 e^+$	$1.1 \cdot 10^{33}$ [40]	-
$p \to K^0 \mu^+$	$3.6 \cdot 10^{33}$ [41]	-
$p \to \pi^+ \overline{\nu}$	$3.9 \cdot 10^{32}$ [42]	-
$p \to K^+ \overline{\nu}$	$6.6 \cdot 10^{33}$ [43]	$3.2 \cdot 10^{34}$ [38]

Table 4: Present experimental bounds on the partial lifetimes τ_p as well as future sensitivities for 10 years of runtime, both at 90% confidence level.

The current experimental constraints and future sensitivities for the various partial lifetimes that are used in the numerical analysis are presented in Table 4.

To start the numerical analysis one first constructs matrices M_e, M_u, Y^a, Y^b, and Y^c at the unification scale, as described in the next few paragraphs.

Namely, since the model yields $E_L = E_R = 1$ and $U_R = U_L^*$, one has that $M_e = \text{diag}(m_e, m_\mu, m_\tau)$ and $M_u = U_L \text{diag}(m_u, m_c, m_t) U_L^T$. The up-type quark mixing matrix U_L can be parametrized in terms of the down-type quark mixing matrix D_L, the Cabibbo-Kobayashi-Maskawa (CKM) matrix $V_{\rm CKM}$, and five phases β_1^u, β_2^u, η_1^u, η_2^u, and η_3^u, as

$$U_L = D_L \text{diag}(e^{i\beta_1^u}, e^{i\beta_2^u}, 1) V_{\rm CKM}^T \text{diag}(e^{i\eta_1^u}, e^{i\eta_2^u}, e^{i\eta_3^u}) \; . \tag{45}$$

In the analysis, one takes $\eta_1^u = \eta_2^u = \eta_3^u = 0$ since these three phases do not affect the proton decay predictions at all.

Y^a and Y^b are constructed via Eq. (30) using matrix $N = \text{diag}(e^{i\eta_1^\nu}, e^{i\eta_2^\nu}, e^{i\eta_3^\nu}) V_{\rm PMNS}^*$ as an input. Note that $V_{\rm PMNS}$ contains the CP violating phase δ^ν as well as the Majorana phase β^ν. Y^c, on the other hand, is a general complex 1×3 matrix

$$Y^c = (y_1^c e^{i\eta_1^c} \quad y_2^c e^{i\eta_2^c} \quad y_3^c e^{i\eta_3^c})^T . \tag{46}$$

Once the parameter dependence of M_u, M_e, Y^a, Y^b, and Y^c is properly accounted for, as described above, one can also construct M_d and M_ν that are given by Eqs. (26) and (28), respectively. λ in M_ν is treated as a free parameter while the two Higgs VEVs that enter M_d and M_ν are given by $v_{\Lambda_1} = v_{\Lambda_2} = 174/\sqrt{2}\,\text{GeV}$ due to the constraint that $\tan\beta$ of Eq. (34) is equal to one.

In summary, the free parameters for the numerical analysis are the unification scale $M_{\rm GUT}$ and the corresponding gauge coupling $\alpha_{\rm GUT}$, the masses of the fields $\phi_3^{\rm Im}$, $\phi_8^{\rm Re}$, $\phi_8^{\rm Im}$, Σ_1, Φ_1, Φ_3, Φ_6, T_1, T_2, and H_2, the phases $\beta_{1,2}^u$, δ^ν, β^ν, $\eta_{1,2,3}^\nu$, the Yukawa parameters $y_{1,2,3}^c$, $\eta_{1,2,3}^c$, the quartic Higgs coupling λ, and the scaling parameter ξ. These 24 parameters are fitted to the experimental observables that are the SM gauge couplings g_1, g_2, and g_3, and the down-type quark masses m_d, m_s, and m_b, while requiring that the current proton decay constraints, as given in Table 4, are satisfied. Note that the charged lepton masses, the up-type quark masses, the neutrino mass squared differences, the CKM mixing parameters, and the known PMNS mixing parameters are all automatically accounted for. For more details on the numerical procedure see Ref. [14].

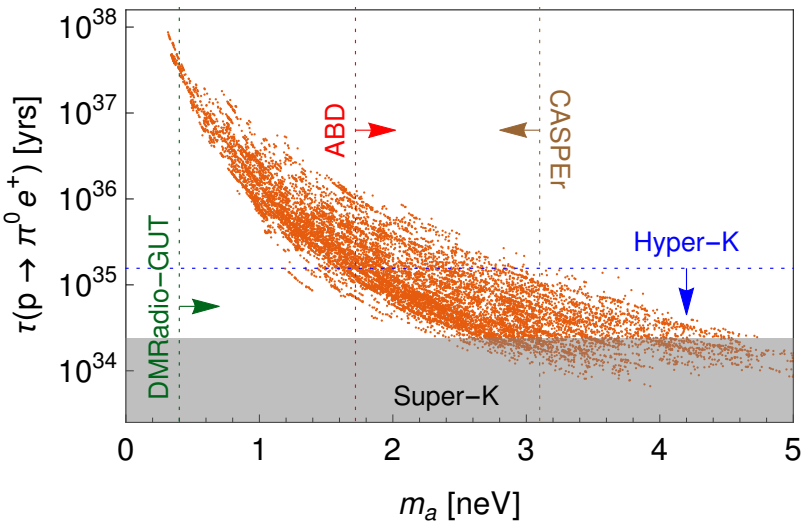

Figure 5: The generated points from the numerical analysis presented in the $m_a - \tau(p \to \pi^0 e^+)$ plane. The current Super-Kamiokande bound is represented by a gray box, while the future Hyper-Kamiokande sensitivity is indicated by a blue dotted line. Moreover, the projected sensitivity of various axion DM experiments is also shown: ABRACADABRA (ABD) with a red dotted line, DMRadio-GUT with a green dotted line, CASPEr Electric with a brown dotted line. For details, see the main text.

The outcome of the numerical analysis is presented in Fig. 5 in a plane of axion mass vs. partial proton decay lifetime in the dominant decay channel $p \to \pi^0 e^+$. There, I also present the future sensitivities of the DM experiments ABRACADABRA, DMRadio-GUT, and CASPEr Electric, as discussed in Sec. 3, as well as the future sensitivity of the proton decay experiment Hyper-Kamiokande.

Fig. 5 nicely visualizes how various parts of the model parameter space can be probed through the synergy between three different kinds of experiments testing (*i*) the axion to photon coupling, (*ii*) the nucleon EDM, and (*iii*) proton decay. For example, if the axion mass is observed to be above 3 neV, proton decay via $p \to \pi^0 e^+$ necessarily has to be seen by Hyper-Kamiokande if this model is realized in nature. Moreover, regardless of whether proton decay will be observed by Hyper-Kamiokande, the former two kinds of experiments will be able to cover the entire parameter space of the model.

The proton decay predictions of all two-body decay channels within the model, for a fixed value of $M_{\rm GUT}$, are shown in Fig. 6, where the blue line segments indicate the current experimental bounds at 90% confidence level presented in Table 4. Fig. 6 is meant to show parameter dependence of different decay channels on the flavor structure in the fermion mass matrices.

Finally, the numerical analysis also yields viable intervals of the Dirac CP and Majorana phase of the PMNS matrix. Namely, it gives $\delta^\nu \in [-22.6°, 34.4°]$ and $\beta^\nu \in [-124.1°, -71.4°]$ at $1\,\sigma$, while the $2\,\sigma$ results are $\delta^\nu \in [-50.7°, 55.6°]$ and $\beta^\nu \in [-132.2°, -54.1°]$.

5. Conclusions

I present a minimal model of unification based on an $SU(5)$ gauge group augmented with a $U(1)$ Peccei-Quinn symmetry that predicts an ultralight axion dark matter with a mass between

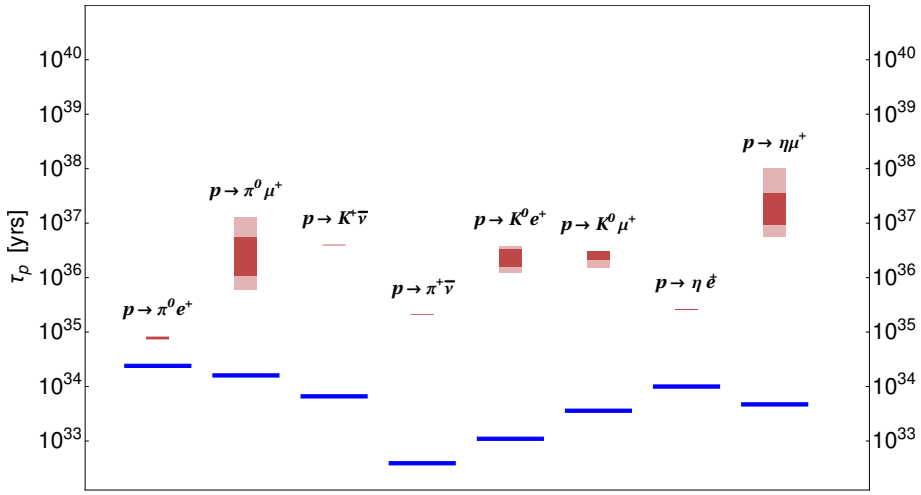

Figure 6: The $1\,\sigma$ (dark) and $2\,\sigma$ (light) intervals of the proton lifetime for various decay channels for a benchmark scenario with $M_{\rm GUT} = 10^{16.2}$ GeV. The blue line segments represent the current experimental bounds at 90% confidence level.

0.1 neV and 4.7 neV. The model also predicts that neutrinos are of Majorana nature, with a normal mass hierarchy spectrum, where one neutrino is massless. The entire parameter space of the model will be tested through a synergy between experiments that look for proton decay and axion dark matter.

References

[1] H. Georgi and S. L. Glashow, Phys. Rev. Lett. **32** (1974), 438-441 doi:10.1103/PhysRevLett.32.438

[2] R. D. Peccei and H. R. Quinn, Phys. Rev. Lett. **38** (1977), 1440-1443 doi:10.1103/PhysRevLett.38.1440

[3] R. D. Peccei and H. R. Quinn, Phys. Rev. D **16** (1977), 1791-1797 doi:10.1103/PhysRevD.16.1791

[4] S. Weinberg, Phys. Rev. Lett. **40** (1978), 223-226 doi:10.1103/PhysRevLett.40.223

[5] F. Wilczek, Phys. Rev. Lett. **40** (1978), 279-282 doi:10.1103/PhysRevLett.40.279

[6] J. E. Kim, Phys. Rev. Lett. **43** (1979), 103 doi:10.1103/PhysRevLett.43.103

[7] M. A. Shifman, A. I. Vainshtein and V. I. Zakharov, Nucl. Phys. B **166** (1980), 493-506 doi:10.1016/0550-3213(80)90209-6

[8] A. R. Zhitnitsky, Sov. J. Nucl. Phys. **31** (1980), 260

[9] M. Dine, W. Fischler and M. Srednicki, Phys. Lett. B **104** (1981), 199-202 doi:10.1016/0370-2693(81)90590-6

[10] J. Preskill, M. B. Wise and F. Wilczek, Phys. Lett. B **120** (1983), 127-132 doi:10.1016/0370-2693(83)90637-8

[11] L. F. Abbott and P. Sikivie, Phys. Lett. B **120** (1983), 133-136 doi:10.1016/0370-2693(83)90638-X

[12] M. Dine and W. Fischler, Phys. Lett. B **120** (1983), 137-141 doi:10.1016/0370-2693(83)90639-1

[13] M. B. Wise, H. Georgi and S. L. Glashow, Phys. Rev. Lett. **47** (1981), 402 doi:10.1103/PhysRevLett.47.402

[14] S. Antusch, I. Doršner, K. Hinze and S. Saad, Phys. Rev. D **108** (2023) no.1, 015025 doi:10.1103/PhysRevD.108.015025 [arXiv:2301.00809 [hep-ph]].

[15] I. Doršner and S. Saad, Phys. Rev. D **101** (2020) no.1, 015009 doi:10.1103/PhysRevD.101.015009 [arXiv:1910.09008 [hep-ph]].

[16] I. Doršner, E. Džaferović-Mašić and S. Saad, Phys. Rev. D **104** (2021) no.1, 015023 doi:10.1103/PhysRevD.104.015023 [arXiv:2105.01678 [hep-ph]].

[17] K. S. Babu, S. Nandi and Z. Tavartkiladze, Phys. Rev. D **80** (2009), 071702 doi:10.1103/PhysRevD.80.071702 [arXiv:0905.2710 [hep-ph]].

[18] G. Bambhaniya, J. Chakrabortty, S. Goswami and P. Konar, Phys. Rev. D **88** (2013) no.7, 075006 doi:10.1103/PhysRevD.88.075006 [arXiv:1305.2795 [hep-ph]].

[19] R. L. Workman *et al.* [Particle Data Group], PTEP **2022** (2022), 083C01 doi:10.1093/ptep/ptac097

[20] I. Cordero-Carrión, M. Hirsch and A. Vicente, Phys. Rev. D **99** (2019) no.7, 075019 doi:10.1103/PhysRevD.99.075019 [arXiv:1812.03896 [hep-ph]].

[21] I. Cordero-Carrión, M. Hirsch and A. Vicente, Phys. Rev. D **101** (2020) no.7, 075032 doi:10.1103/PhysRevD.101.075032 [arXiv:1912.08858 [hep-ph]].

[22] M. Srednicki, Nucl. Phys. B **260** (1985), 689-700 doi:10.1016/0550-3213(85)90054-9

[23] L. Di Luzio, M. Giannotti, E. Nardi and L. Visinelli, Phys. Rept. **870** (2020), 1-117 doi:10.1016/j.physrep.2020.06.002 [arXiv:2003.01100 [hep-ph]].

[24] W. A. Bardeen, S. H. H. Tye and J. A. M. Vermaseren, Phys. Lett. B **76** (1978), 580-584 doi:10.1016/0370-2693(78)90859-6

[25] G. Grilli di Cortona, E. Hardy, J. Pardo Vega and G. Villadoro, JHEP **01** (2016), 034 doi:10.1007/JHEP01(2016)034 [arXiv:1511.02867 [hep-ph]].

[26] Y. Kahn, B. R. Safdi and J. Thaler, Phys. Rev. Lett. **117** (2016) no.14, 141801 doi:10.1103/PhysRevLett.117.141801 [arXiv:1602.01086 [hep-ph]].

[27] V. Domcke, C. Garcia-Cely and N. L. Rodd, Phys. Rev. Lett. **129** (2022) no.4, 041101 doi:10.1103/PhysRevLett.129.041101 [arXiv:2202.00695 [hep-ph]].

[28] C. Murgui, Y. Wang and K. M. Zurek, Phys. Lett. B **855** (2024), 138832 doi:10.1016/j.physletb.2024.138832 [arXiv:2211.08432 [hep-ph]].

[29] C. B. Adams, N. Aggarwal, A. Agrawal, R. Balafendiev, C. Bartram, M. Baryakhtar, H. Bekker, P. Belov, K. K. Berggren and A. Berlin, *et al.* [arXiv:2203.14923 [hep-ex]].

[30] D. Budker, P. W. Graham, M. Ledbetter, S. Rajendran and A. Sushkov, Phys. Rev. X **4** (2014) no.2, 021030 doi:10.1103/PhysRevX.4.021030 [arXiv:1306.6089 [hep-ph]].

[31] D. F. Jackson Kimball, S. Afach, D. Aybas, J. W. Blanchard, D. Budker, G. Centers, M. Engler, N. L. Figueroa, A. Garcon and P. W. Graham, *et al.* Springer Proc. Phys. **245** (2020), 105-121 doi:10.1007/978-3-030-43761-9_13 [arXiv:1711.08999 [physics.ins-det]].

[32] P. W. Graham and S. Rajendran, Phys. Rev. D **88** (2013), 035023 doi:10.1103/PhysRevD.88.035023 [arXiv:1306.6088 [hep-ph]].

[33] M. Pospelov and A. Ritz, Phys. Rev. Lett. **83** (1999), 2526-2529 doi:10.1103/PhysRevLett.83.2526 [arXiv:hep-ph/9904483 [hep-ph]].

[34] G. Ballesteros, J. Redondo, A. Ringwald and C. Tamarit, JCAP **08** (2017), 001 doi:10.1088/1475-7516/2017/08/001 [arXiv:1610.01639 [hep-ph]].

[35] N. Aghanim *et al.* [Planck], Astron. Astrophys. **641** (2020), A6 [erratum: Astron. Astrophys. **652** (2021), C4] doi:10.1051/0004-6361/201833910 [arXiv:1807.06209 [astro-ph.CO]].

[36] S. Antusch and V. Maurer, JHEP **11** (2013), 115 doi:10.1007/JHEP11(2013)115 [arXiv:1306.6879 [hep-ph]].

[37] A. Takenaka *et al.* [Super-Kamiokande], Phys. Rev. D **102** (2020) no.11, 112011 doi:10.1103/PhysRevD.102.112011 [arXiv:2010.16098 [hep-ex]].

[38] K. Abe *et al.* [Hyper-Kamiokande], [arXiv:1805.04163 [physics.ins-det]].

[39] K. Abe *et al.* [Super-Kamiokande], Phys. Rev. D **96** (2017) no.1, 012003 doi:10.1103/PhysRevD.96.012003 [arXiv:1705.07221 [hep-ex]].

[40] R. Brock, C. K. Jung, C. E. M. Wagner, K. S. Babu, R. Dermisek, B. Dutta, P. Fileviez Perez, K. S. Ganezer, I. Gogoladze and Y. Kamyshkov, *et al.*

[41] R. Matsumoto *et al.* [Super-Kamiokande], Phys. Rev. D **106** (2022) no.7, 072003 doi:10.1103/PhysRevD.106.072003 [arXiv:2208.13188 [hep-ex]].

[42] K. Abe *et al.* [Super-Kamiokande], Phys. Rev. Lett. **113** (2014) no.12, 121802 doi:10.1103/PhysRevLett.113.121802 [arXiv:1305.4391 [hep-ex]].

[43] V. Takhistov [Super-Kamiokande], [arXiv:1605.03235 [hep-ex]].